

Catheter Ablation of Ventricular Tachycardia After Repair of Congenital Heart Disease

Electroanatomic Identification of the Critical Right Ventricular Isthmus

Katja Zeppenfeld, MD; Martin J. Schalij, MD; Margot M. Bartelings, MD; Usha B. Tedrow, MD; Bruce A. Koplán, MD; Kyoko Soejima, MD; William G. Stevenson, MD

Background—Catheter ablation of ventricular tachycardia (VT) after repair of congenital heart disease can be difficult because of nonmappable VTs and complex anatomy. Insights into the relation between anatomic isthmuses identified by delineating unexcitable tissue using substrate mapping techniques and critical reentry circuit isthmuses might facilitate ablation.

Methods and Results—Sinus rhythm voltage mapping of the right ventricle was performed in 11 patients with sustained VT after repair of congenital heart disease. Unexcitable tissue from patch material, valve annulus, or dense fibrosis, identified from bipolar voltage (<0.5 mV) and pacing threshold (>10 mA), was defined as an anatomic isthmus boundary bordering 4 isthmuses between (1) the tricuspid annulus and scar/patch in the anterior right ventricular outflow, (2) the pulmonary annulus and right ventricular free wall scar/patch, (3) the pulmonary annulus and septal scar/patch, and (4) the septal scar/patch and tricuspid annulus. The reentry circuit isthmuses of all induced 15 VTs (mean cycle length, 276 ± 78 ms; 73% poorly tolerated), identified by activation, entrainment, and/or pace mapping, were located in an anatomic isthmus (11 of 15 VTs in anatomic isthmus 1). Transecting the anatomic isthmuses by ablation lesions abolished all VTs. During 30.4 ± 29.3 months of follow-up, 91% of patients remained free of VT.

Conclusions—Reentry circuit isthmuses in VT late after repair of congenital heart disease are located within anatomically defined isthmuses bordered by unexcitable tissue. The boundaries can be identified with 3-dimensional substrate mapping and connected by ablation lines during sinus rhythm. These findings should facilitate catheter and surgical ablation of stable and unstable VTs. (*Circulation*. 2007;116:2241-2252.)

Key Words: catheter ablation ■ heart defects, congenital ■ tachyarrhythmias

Surgical treatment has improved the long-term prognosis of patients with congenital heart disease (CHD), but late ventricular arrhythmias remain a risk for patients who have had ventriculotomies.^{1,2} After repair of tetralogy of Fallot (TOF), the incidence of ventricular tachycardia (VT) is 11.9%, with an 8.3% risk of sudden death by 35 years of follow-up.³ Case reports and small series of intraoperative and catheter mapping have demonstrated reentry as the underlying mechanism of these VTs, although other causes cannot be excluded.⁴⁻⁷ The feasibility of catheter ablation, applying conventional mapping techniques, has been reported.⁸ However, complex anatomy, hypertrophied myocardium, broad isthmuses, hemodynamic instability, or noninducibility of the VTs may explain ablation failure in 50% of cases.^{9,10}

Editorial p 2236 Clinical Perspective p 2252

Anatomic regions of conduction block that can potentially define critical isthmuses for reentry include valve annuli,

patch material, and surgical incisions. Recently, methods to better characterize the reentry substrate by defining areas of block or unexcitable scar on 3-dimensional (3D) maps during sinus rhythm (SR) have been applied to other types of scar-related reentry.^{11,12}

We hypothesized that substrate mapping techniques provide a 3D reconstruction of anatomic isthmuses after repair of CHD and that pace mapping within these anatomic isthmuses provides a potential indication of the reentry circuit exit location. These methods might then allow ablation strategies designed to transect critical isthmuses during SR.

Methods

Patients

Review of medical records was approved by the Brigham and Women's Hospital human subject protection committee. Eleven consecutive patients (8 men; age, 43.7 ± 10.6 years) with recurrent symptomatic VT after repair of CHD who were referred to 2 centers (Brigham and Women's Hospital and Leiden University Medical Center) for radiofre-

Received June 25, 2007; accepted August 22, 2007.

From the Departments of Cardiology and Anatomy, Leiden University Medical Center, Leiden, the Netherlands (K.Z., M.J.S., M.M.B.), and the Cardiovascular Division, Brigham and Women's Hospital, Boston, Mass (U.B.T., B.A.K., K.S., W.G.S.).

Guest Editor for this article was Douglas P. Zipes, MD.

Correspondence to Katja Zeppenfeld, MD, Leiden University Medical Center, PO Box 9600, 2300 RC Leiden, the Netherlands. E-mail k.zeppenfeld@lumc.nl

© 2007 American Heart Association, Inc.

Circulation is available at <http://circ.ahajournals.org>

DOI: 10.1161/CIRCULATIONAHA.107.723551

Table 1. Patient Characteristics

Patient	Age, y	Sex	CHD	Operation	Age at Surgery, y	Symptoms/ Documented Arrhythmia	Baseline QRS, ms	RV Dilatation/ RV EDVI, mL/m ² *	RVOT/PA Peak Gradient, mm Hg	PI	TI	LVEF, %	AAD
1	57	F	TOF	Blalock-Taussig shunt	2	Presyncope/ nsVT	220	Severe, 174.6	None	Mild	Moderate	55	Amiodarone
				Repair, RVI	16								
2	59	M	TOF	Repair, RVI	13	Syncope/ Resuscitation	100	Moderate, 150	None	Moderate	Moderate	50	Sotalol
3	36	F	TOF	Waterston shunt	1	Presyncope/ sVT	145	Mild, 127.7	None	Mild	None	60	None
				Repair, TAP	7								
				PVR	35								
4	48	F	TOF	Blalock-Taussig shunt	1	Syncope/sVT	200	Mild, 109.4	16	Mild	Mild	65	Amiodarone
				Repair, TAP	9								
				PVR	42								
5	50	M	TOF	Repair, TAP	9	Palpitation/ sVT	160	Mild	9	None	Mild	60	Amiodarone
6	33	M	TOF	Repair, RVOTP	10	Palpitation/ sVT	106	Mild	30	Moderate	Mild	60	Sotalol
7	42	M	TOF	Blalock-Taussig shunt	2	Palpitation/ sVT	195	Moderate 141.8	8	None	None	60	Sotalol
				Repair, RVI	10								
				PV	14								
				valvuloplasty, TAP, ASD closure									
8	38	M	TOF	Blalock-Taussig shunt	1.5	Presyncope/ sVT	160	Mild	20	None	None	60	Metoprolol
				Waterston shunt	8								
				Repair, RVI	10								
9	23	M	TGA, VSD	Arterial switch, RVI, VSD closure	0.8	Palpitation/ sVT	155	Mild	14	None	None	60	None
10	49	M	In-complete AVSD	ASD and VSD closure, mitral valvuloplasty	25	Palpitation/ sVT	160	Severe	None	Mild	Moderate	60	None
11	46	M	TOF	Repair, RVI	11	Syncope/sVT	105	Mild	11	Mild	Mild	65	Sotalol

EDVI indicates end-diastolic volume index; PA, pulmonary artery; PI, pulmonary insufficiency; TI, tricuspid insufficiency; LVEF, left ventricular ejection fraction; AAD, antiarrhythmic drugs; nsVT, nonsustained VT; RVI, RV incision; sVT, sustained VT; TAP, transannular patch; PVR, pulmonary valve replacement; RVOTP, RVOT patch; ASD, atrial septum defect; TGA, transposition of the great arteries; and AVSD, atrioventricular septal defect.

*Magnetic resonance imaging data.

quency (RF) catheter ablation were investigated between February 1998 and January 2007 (9 of 11 were included after February 2004) (Table 1). Patient 8 has been previously reported.⁷

Nine patients had undergone surgical repair of TOF at an average age of 10.5 ± 2.6 years; 1 patient had repair of an atrioventricular septal defect by patch closure of an ostium primum atrial septal defect and

patch closure of an inlet ventricular septal defect (VSD). The remaining patient had d-transposition of the great arteries associated with VSD without significant pulmonary stenosis that was corrected by an arterial switch operation and patch closure of the VSD.

Three TOF patients had undergone a second operation (pulmonary valve replacement in 2, valvuloplasty in 1). VT occurred at a mean of

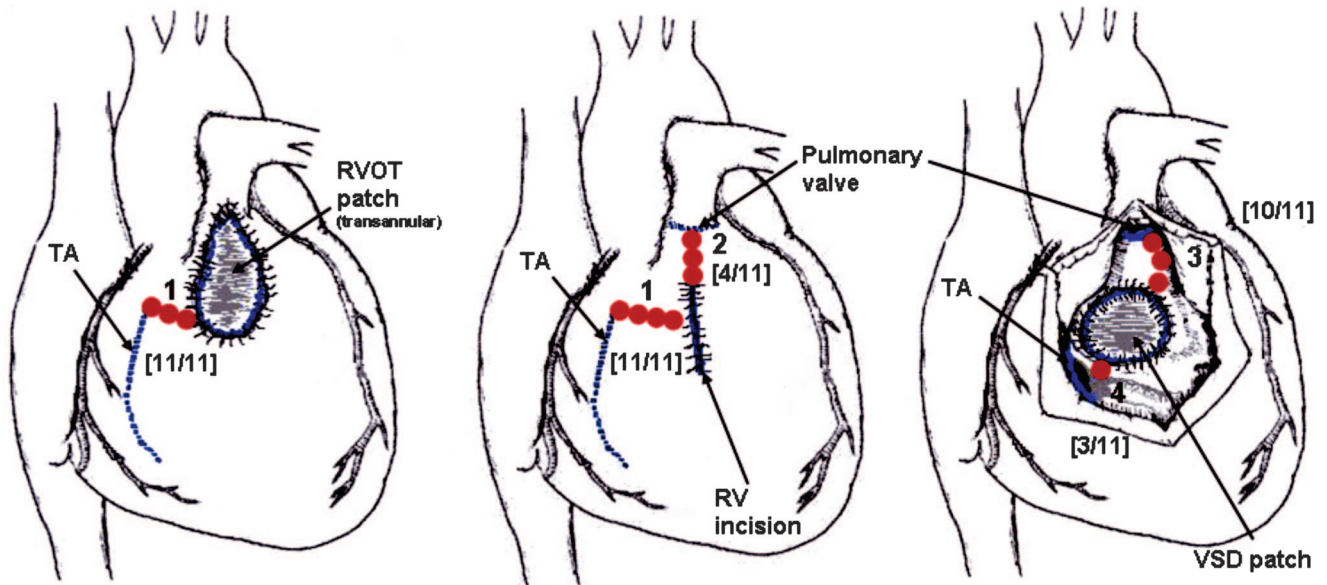


Figure 1. Schematic of the localization of anatomic boundaries (blue lines) for VT after repair of CHD and the resulting anatomic isthmuses (red lines); frequency of the distinct isthmuses in brackets.

34.3±7.6 years after surgical correction. Three patients had recurrent syncope; 1 had been resuscitated after VT degenerated to VF. Three patients had recurrent presyncope, 2 with documented sustained VT and 1 with nonsustained VTs on a Holter recording. The remaining 5 patients had palpitations and documented sustained VT.

Mean QRS duration on the resting ECG of TOF patients was 154±44 ms (range, 100 to 220 ms). Echocardiography was performed in all patients; 5 underwent cardiac magnetic resonance imaging, and 1 had multislice computed tomography imaging.

The right ventricle (RV) was mildly dilated in 7, moderately dilated in 2, and severely dilated (RV inlet >60 mm) in 2 patients, with severely reduced function in 1 patient. Left ventricular function was preserved in all patients (mean ejection fraction, 59±5%). Pulmonary regurgitation was moderate (20% to 40% on magnetic resonance imaging) in 2 patients, and a moderate pressure gradient across the RV outflow tract (RVOT) was evident in 1 patient.¹³

Electrophysiological Study and Mapping

After informed consent was obtained, conscious sedation was achieved with fentanyl and midazolam. Electrode catheters were positioned in the RV, His-bundle position, and right atrium via femoral veins. Bipolar signals (filtered at 30 to 400 Hz) and 12-lead ECGs were stored on optical disks for offline analysis (Prucka Engineering, GE Healthcare, Piscataway, NJ).

Programmed stimulation was performed from the RV apex and RVOT (3 extrastimuli, 3 basic cycle lengths [CLs]) to induce VT and to obtain the QRS morphology. VTs with a predominantly positive deflection in lead V₁ were considered right bundle-branch block morphology tachycardias; those with a predominantly negative deflection in V₁ were considered left bundle-branch block morphology tachycardias.

RV mapping during SR was performed with a 3.5-, 4-, or 8-mm-tip catheter with 1-mm (Navi-Star) or 2-mm (Thermocool) interelectrode spacing of the recording electrodes (Thermocool, Navi-Star 4 mm, Navi-Star 8 mm; Biosense Webster, Inc; Diamond Bar, Calif) to construct a 3D voltage map using an electroanatomic mapping system (CARTO; Biosense Webster). Peak-to-peak bipolar amplitudes were displayed color coded, with electrograms <1.5 mV defined as low voltage and electrograms <0.5 mV as very low-voltage electrograms on the basis of mapping data obtained in patients without structural heart disease.¹¹ At low-amplitude sites, unipolar pacing was performed with 10 mA at a 2-ms pulse width between the distal electrode of the ablation catheter (negative pole)

and an indifferent electrode (positive pole) located remote from the heart in the inferior vena cava. Sites with pacing threshold >10 mA were tagged as electrically unexcitable scar (EUS) and were shown as gray regions.¹² The His-bundle position was marked and the pulmonary valve was localized by advancing the catheter into the pulmonary artery and withdrawing it until an RV electrogram was identified. When the valve was not located in patients with transannular patches and/or adjacent RVOT scar, these regions also were tagged as scar if pacing did not capture. Anatomic boundaries were defined as EUS, pulmonary valve, tricuspid annulus (TA), or very low-voltage electrograms; anatomic isthmuses were defined as areas between these boundaries.

Identification of VT Circuits

After voltage mapping, VT was reinduced. In patients with tolerated VT, activation and entrainment mapping was performed. Reentry circuit isthmus sites were defined by entrainment showing either concealed fusion with a difference between the postpacing interval and the VTCL of ≤30 ms and a stimulus to QRS distance (S-QRS) of ≤70% of the VTCL or sites with diastolic electrical activity during VT and termination and prevention of reinitiation of VT by RF ablation. For VTs that were not mappable because of hemodynamic instability or termination during catheter manipulation or entrainment mapping, reentry circuit isthmuses were defined by pace mapping at sites where the QRS morphology matched that of the VT (≥10 of 12 leads) with an S-QRS delay of >40 ms. If VT could be briefly tolerated, the catheter was moved to the presumed isthmus site during SR, and the VT was reinduced to confirm the position within the circuit either by entrainment mapping or by termination during RF delivery.

Catheter Ablation

RF ablation was performed with an open saline-irrigated catheter (power limit, 50 W) in 8 patients (Thermocool), a closed irrigation catheter in 1 patient (Chilli, Boston Scientific, Natick, Mass), and an 8-mm-tip catheter (power limit, 70 W) in 2 patients (Navi-Star, 8 mm). VT isthmuses were targeted for ablation. Ablation was performed during VT when possible. If VT terminated or slowed during RF application, additional lesions were placed to connect the adjoining anatomic boundaries. In patients with poorly tolerated VT, pace mapping was used to select isthmus sites. RF lesions were placed during SR until unipolar pacing failed to capture. After completion of the lesions, programmed stimulation was repeated,

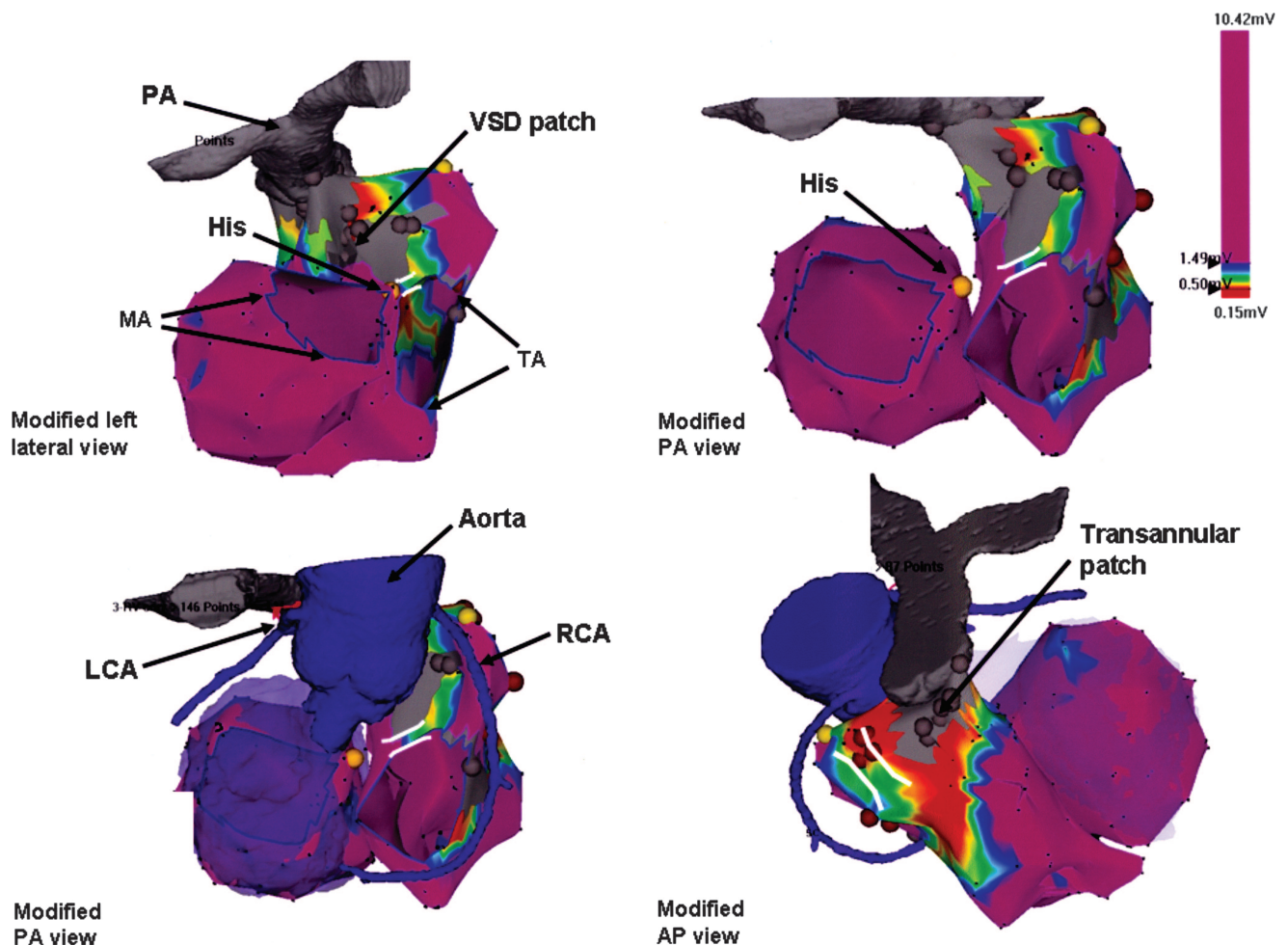


Figure 2. Voltage maps of the left ventricle and RV merged with a computed tomography scan in a patient after repair of TOF (patient 4). Red areas have an electrogram amplitude <0.5 mV; purple areas, >1.5 mV. Gray areas indicate sites of EUS. Anatomic isthmuses are indicated by white lines. The yellow tag indicates the His position; note the vicinity of the His position and isthmus 4 between the septal scar and the TA. No area of excitable myocardium was found between the RVOT scar and pulmonary valve. Note the clockwise rotation (viewed from below) of the aorta, resulting in a leftward displacement of the right coronary cusp, typical for TOF. Linear ablation lesions (red tags) extend across the anatomic isthmus. PA indicates pulmonary artery; MA, mitral annulus; RCA, right coronary artery; and LCA, left coronary artery.

including during isoproterenol infusion (1 to 8 $\mu\text{g}/\text{min}$). If any monomorphic VT was inducible, the mapping and ablation process was repeated. Successful VT ablation was defined as the absence of any inducible sustained (>30 seconds or requiring termination) monomorphic VT.

Morphology of Postmortem Specimens After Repair of TOF

From the Leiden collection of malformed hearts, 8 postmortem specimens with repaired TOF were studied to examine the variation in morphology after corrective surgery and the distribution and number of anatomic isthmuses. The 8 patients (4 male) died at a mean age of 4.1 years (range, 0.4 to 10.4 years). Seven patients died within 11 days after repair; 1 patient survived 5.0 years.

The authors had full access to and take full responsibility for the integrity of the data. All authors have read and agree to the manuscript as written.

Results

Anatomic Isthmuses

SR voltage maps of the RV were constructed from an average of 224 ± 69 sites per patient (range, 162 to 317). RVOT sites

showed widespread low-voltage signals indicating abnormal myocardium. Within these low-voltage regions, areas of EUS were identified in the 10 patients tested for EUS; in patient 8 (studied in 1998), isthmus boundaries were defined as areas with very low-voltage electrograms (<0.5 mV).

EUS in a septal location was present in all patients; in 8 patients, the septal EUS was in continuity with the TA. Two additional patterns of EUS could be identified. The first showed EUS of the anterior RVOT in continuity with the pulmonary valve. Patients 3, 4, 5, and 7 who had undergone transannular patch repair, patient 6 with RVOT patch, and patient 1 with resection of a subpulmonary stenosis via RV incision showed this pattern. The second pattern showed EUS of the anterior RVOT or adjacent RV free wall separated from the pulmonary valve by an intervening area where pacing captured. This pattern was found in patients 2, 8, 10, and 11; all had operative correction by an RV incision. The distribution of border-forming areas resulted in 4 distinct anatomic isthmuses located between the RVOT/adjacent RV scar and TA (isthmus 1) found in all patients, between the RV scar and pulmonary valve (isthmus 2)

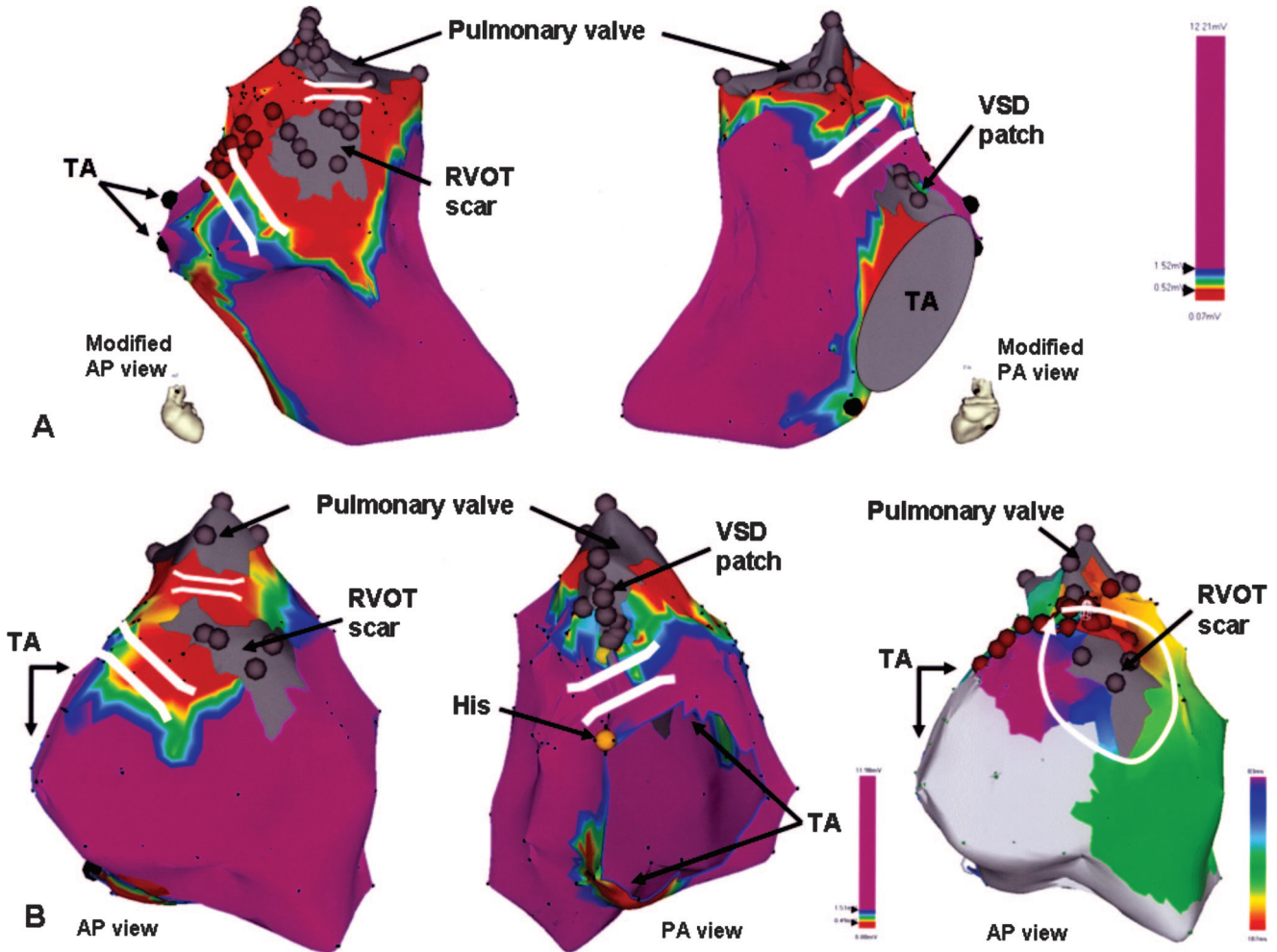


Figure 3. A, Voltage maps of RV in a modified anterior (AP) view and modified posterior (PA) view (TOF; patient 2). Three anatomic isthmuses could be delineated (white lines). In this patient, 1 isthmus is bordered by the pulmonary valve and RVOT scar. No muscular rim is present between the VSD patch and the TA. Linear ablation lesions (red tags) transect anatomic isthmus 1. B, Voltage maps of RV in an AP view (left) and PA view (center) (TOF; patient 11). In contrast to patient 2, a muscular rim is present between the VSD patch and the TA. Activation map of VT 3 (right, AP view). Activation time is color coded; the activation time (270 ms) equals the VTCL. The macroreentrant circuit propagates clockwise around the RVOT scar through isthmus 2 and inferior to superior through isthmus 1. The catheter tip indicates the termination site. In the same patient, the anatomic isthmus between the TA and the RVOT scar also was transected, resulting in noninducibility of all 3 VTs.

in 4 patients, between the pulmonary valve and septal scar (isthmus 3) in 10 patients, and between the septal scar and TA (isthmus 4) in 3 patients (Figure 1). Figure 2 gives an example of anatomic isthmus 1 and 4 identified by 3D voltage mapping; Figure 3A and 3B shows isthmus 1, 2, and 3 and isthmus 1, 2, and 4, respectively.

Distribution of the Anatomic Isthmuses in Postmortem Specimens

Seven of the 8 specimens had a transannular patch. In 1 specimen, an RVOT patch showed fibrous continuity with the pulmonary valve; thus, no specimen had anatomic isthmus 2 (Figure 4). All specimens had muscular continuity between the transannular/RVOT patch and the TA (isthmus 1), and 7 had muscular continuity between the VSD patch and the pulmonary valve (isthmus 3). In 1 specimen, the VSD patch was bordered by fibrous tissue of the TA and the pulmonary valve excluding anatomic isthmus 3 and 4. Only 1 specimen

had closure of a VSD, leaving a small posterior rim of myocardium compatible with anatomic isthmus 4.

ECG Characteristics of the Induced VTs

In 11 patients, 15 different monomorphic VTs (mean CL, 276±78 ms; range, 202 to 504 ms) could be induced; 9 were documented as spontaneous VTs. In patient 5, the spontaneous VT could not be induced. Thirteen VTs had left bundle-branch-block, and 2 had right bundle-branch block morphologies. Frontal plane axis was left inferior in 11, right inferior in 3, and left superior in 1; precordial transition was at V₂ in 2, V₃ in 6, V₄ in 1, V₅ in 5, and V₆ in 1 (Table 2).

Reentry Circuit Isthmuses Defined by Entrainment, Pace Mapping, and Ablation

Two of the 15 induced VTs were hemodynamically unstable. Nine VTs were briefly tolerated, allowing limited activation and entrainment mapping, with RF application during ongo-

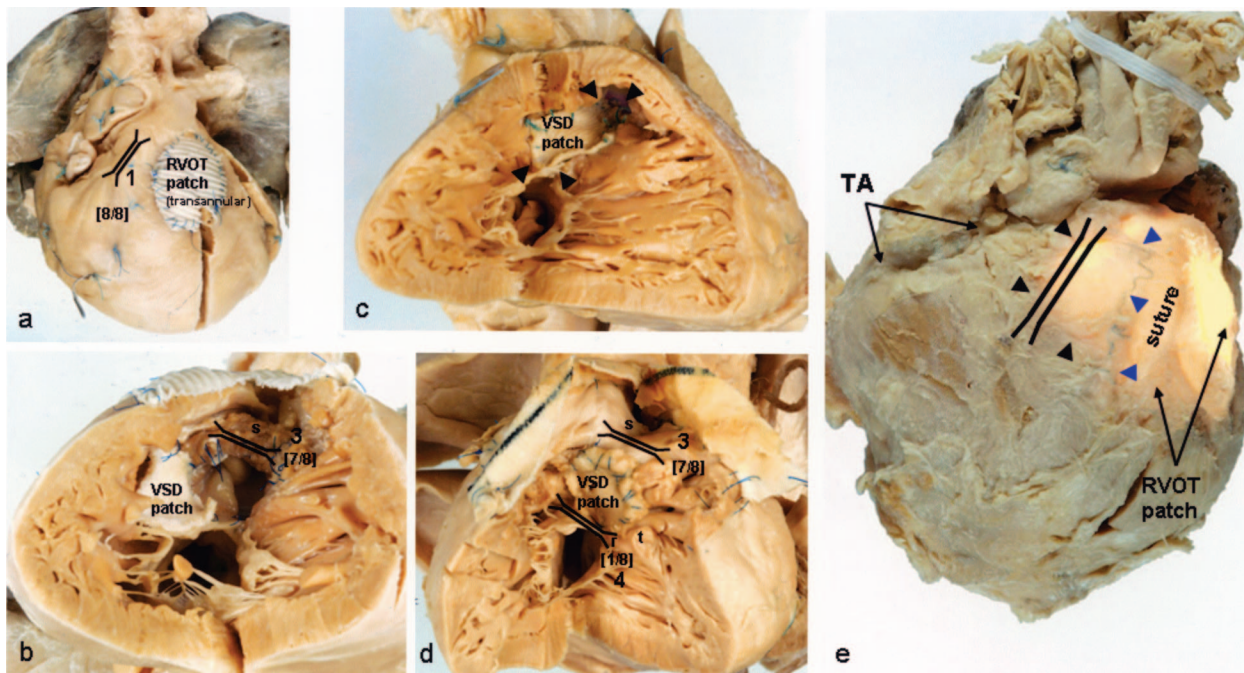


Figure 4. Postmortem specimens with previous repair of TOF shown in an anterior view (a and e) and an RV view (b through d). b, The VSD patch is folded down to demonstrate the perimembranous VSD and the anterocephalad location of the outlet septum. c, Fibrous continuity (arrowheads) between the TA, VSD patch, and pulmonary valve excluding isthmus 3 and 4. d, A small infero-posterior muscular rim (r) of the VSD. e, The heart from a patient who survived 5 years after repair of TOF illuminated from inside. The diaphanous areas represent the transannular patch (blue arrowheads indicate the suture) and the adjacent anterolateral RVOT (black arrowheads), consistent with a location within anatomic isthmus 1. Note the thinning of the anterolateral RVOT. s indicates outlet septum; t, trabecula septomarginalis.

ing VT in only 3 patients. The remaining 4 VTs were well tolerated for mapping and ablation.

Eleven VTs had a reentry circuit isthmus located in anatomic isthmus 1, 1 VT in anatomic isthmus 2, 2 VTs in

anatomic isthmus 3, and 1 VT in anatomic isthmus 4. In all but 1 patient, slow conduction within these anatomic isthmuses was evident as a prolonged S-QRS interval exceeding 40 ms during pace mapping (Table 2).¹⁴

Table 2. ECG Characteristics, Mapping, and Ablation Data

Patient	VT, n	VTCL, ms	Lead V ₁ , LB, RB	Axis	QRS Transition	Stable	Clinical VT	Anatomic Isthmuses	Localization of Reentry Isthmus (Anatomic Isthmus), n	Definition of Reentry Circuit Isthmus Based on			
										Entrainment Mapping: PPI/S-QRS, ms	Pace Mapping: Lead Match; S-QRS, ms	RF Terminates VT	RF Applications No.
1	1	290	LB	LI	V ₅	No	No	1/3	1	...	11/12; 120	...	18
2	1	240	LB	LI	V ₅	No	Yes	1/2/3	1	...	11/12; 65	...	12
3	1	211	LB	LI	V ₃	Briefly	Yes	1/3	1	...	12/12; 45	Yes	4
4	1	386	LB	LS	V ₆	Yes	Yes	1/4	1	390/160	...	Yes	7
5	1	300	LB	LI	V ₅	Yes	No	1/3	1	298/60	26
6	1	240	LB	LI	V ₂	Briefly	Yes	1/3/4	3	227/25	12
	2	270	LB	LI	V ₂	Briefly	No		4	276/45	7
7	1	243	LB	LI	V ₃	Briefly	No	1/3	1	240/93	24
	2	251	LB	LI	V ₅	Briefly	Yes		1	...	11/12; 46	...	
8	1	295	RB	RI	V ₃	Yes	Yes	1/2/3	1	295/105	...	Yes	23
9	1	202	LB	RI	V ₃	Briefly	Yes	1/3	3	...	12/12; 42	Yes	8
10	1	504	LB	LI	V ₃	Yes	Yes	1/2/3	1	504/80	...	Yes	6
11	1	229	LB	LI	V ₄	Briefly	Yes	1/2/3/4	1	...	12/12; 50	...	12
	2	220	LB	LI	V ₅	Briefly	No		1	230/40	...	Yes	
	3	260	RB	RI	V ₃	Briefly	No		2	...	11/12; 55	Yes	8

LB indicates left bundle block; RB, right bundle block; PPI, postpacing interval; LI, left inferior; RI, right inferior; and LS, left superior.

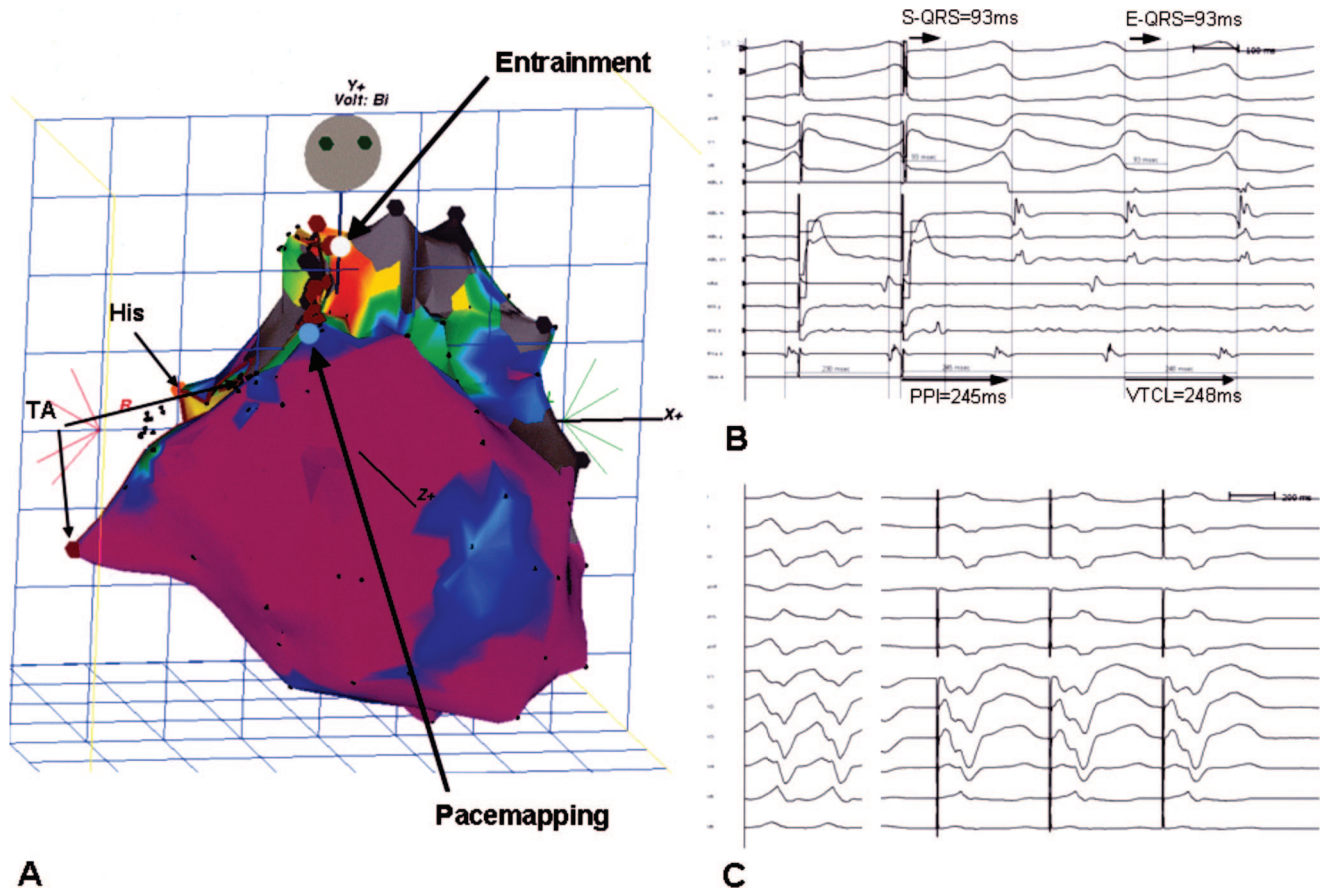


Figure 5. A, Voltage map of the RV (TOF; patient 7). An anatomic isthmus is bordered by scar adjacent to the pulmonary valve and TA. B, During VT1, pacing within an anatomic isthmus (site indicated by a white tag) entrains tachycardia with concealed fusion. The post-pacing interval equals VTCL. The S-QRS is 93 ms, suggesting a central isthmus site. C, VT2 was not stable (12-lead ECG shown on the left). Pace mapping demonstrates a good match of the QRS morphology at the site marked with a blue tag. The short S-QRS indicates a potential exit site of VT, suggesting a superior-to-inferior propagation of the VT wave front.

In patients 3, 9, and 11 (VT3), a reentry isthmus site was identified on the basis of pace mapping during SR and limited VT activation mapping and located within anatomic isthmus 1, 3, and 2, respectively. Activation mapping of VT in patient 3 and VT3 in patient 11 showed a wave front propagating through isthmus 1 in an inferior-to-superior direction. The latter revolved clockwise around the RVOT scar (Figure 3). All 3 VTs were terminated during RF application. Additional RF lesions were applied to connect the boundaries of the anatomic isthmus.

Entrainment mapping demonstrated a central isthmus site in patients 4 and 8 and an exit site in patients 10 and 11 (VT2), all located within isthmus 1. The wave front propagated from superior to inferior through this isthmus in patient 4 and from inferior to superior in patients 8, 10, and 11. Slowing of the VTs occurred during RF delivery at the isthmus site without a change in the QRS morphology. Consecutive RF lesions were applied to connect the initial site of RF delivery to the anatomic boundaries. This resulted in VT termination in the 4 patients. The reentry circuit isthmus of VT1 in patient 11 was localized to isthmus 1 on the basis of pace mapping; this VT was not inducible after these boundaries were connected.

In the remaining 5 patients, RF current was applied only during SR. Localization of reentry circuit isthmuses was based on pace mapping (patients 1 and 2), limited entrainment mapping suggesting an exit site (patients 5 and 6), or both techniques (patient 7) (Figure 5). The site was located within anatomic isthmus 1 in patients 1, 2, 3, and 7; isthmus 3 for VT1, and isthmus 4 for VT2 of patient 6. RF ablation through these isthmuses abolished all 7 VTs. In patient 7, VT1 remained inducible after RF applications within isthmus 1. However, the RVOT/TA line was completed only after a change to an irrigated ablation catheter, which then rendered both VTs not inducible. After completion of these ablation lines with an average of 12.6 ± 7.2 RF lesions (range, 4 to 26), no monomorphic VT was inducible in all patients.

ECG Correlations

Although reentry circuit isthmuses of 11 of 15 VTs were localized within anatomic isthmus 1, QRS configuration was heterogeneous, and the number of VTs was too small for reliable statistical comparisons. Figure 6 gives 1 ECG example for each axis and transition zone of the VTs sharing isthmus 1 and of the VTs mapped to the anatomic isthmus 2, 3, and 4. The precordial transition tended to be at V_3 or later

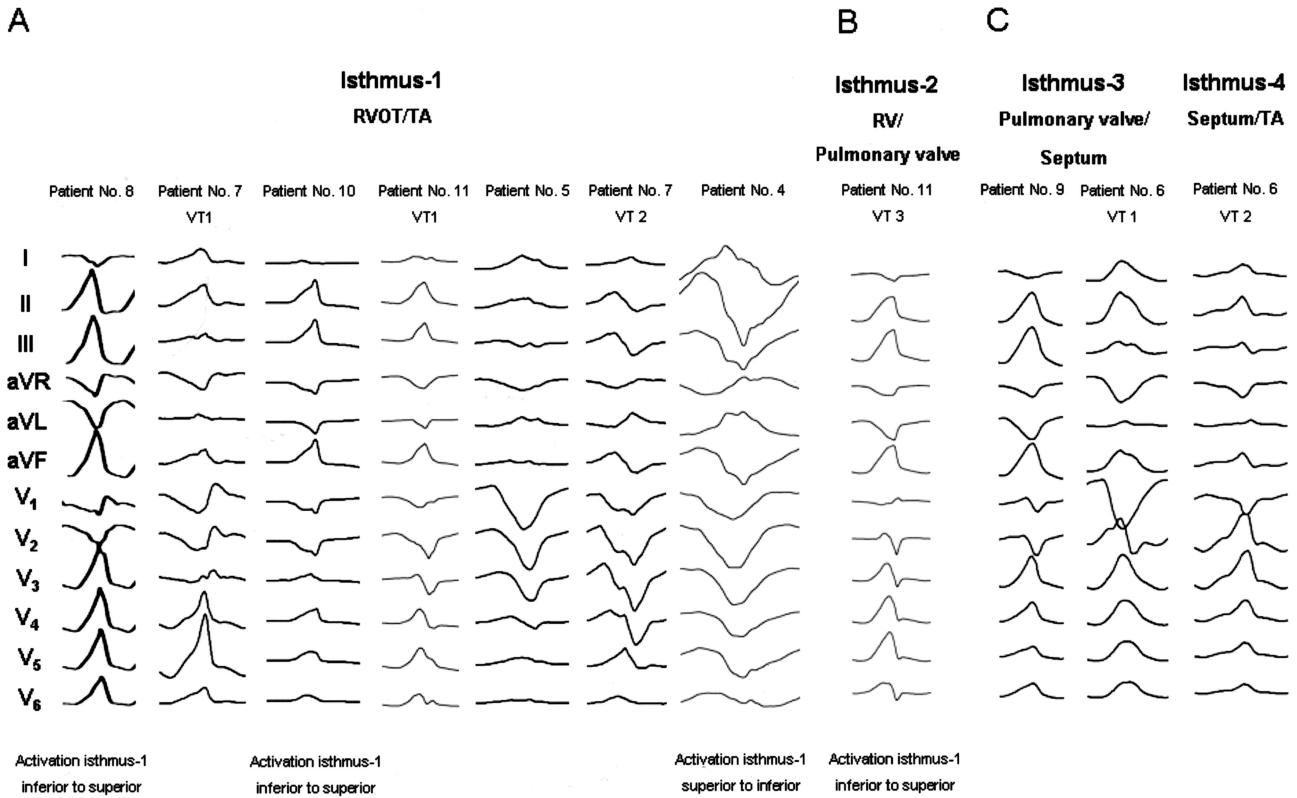


Figure 6. A, Examples of ECGs of VTs sharing anatomic isthmus 1. B, ECG of the VT revolving around the RVOT scar in a clockwise manner using isthmus 2. Note the similarity to the VT in patient 8. C, ECGs of the 3 VTs mapped to isthmus 3 and 4. Note the early precordial transition.

in isthmus 1 VTs but earlier in VTs that used an isthmus bordering on the septum. Furthermore, VTs with an inferior-to-superior wave-front propagation tended to have an earlier precordial transition. The 2 right bundle-branch block VTs propagated from inferior to superior through isthmus 1 and clockwise through isthmus 2. However, the critical isthmus was in isthmus 1 in patient 8 and in isthmus 2 in patient 11.

Patient Follow-Up

No complications occurred. Drug therapy was maintained in 5 patients during follow-up (2 amiodarone, 3 sotalol) and discontinued in 2 (side effects in 1, decision of the referring physician in 1); antiarrhythmic drugs were not administered to 4 patients who were not receiving antiarrhythmic drugs at referral. Nine patients received aspirin (100 to 325 mg for 6 weeks); 2 patients continued anticoagulation with warfarin. During long-term follow-up, 5 patients had implantable cardioverter-defibrillators. Three patients underwent implantation of an implantable cardioverter-defibrillator after ablation (patient 2 after being resuscitated, patient 4 after syncope not explained by the induced stable VT, and patient 3 on request of the referring physician); 1 patient (patient 11) had undergone implantable cardioverter-defibrillator implantation before referral after syncope as a result of a documented fast VT (CL, 230 ms). Three patients had a second study. Patients 8 and 9, who were asymptomatic, had no inducible VT 2 days and 6 months after the initial procedure. Patient 7, who had

recurrence of palpitations but no documented VT, had inducible VT1 (CL, 243 ms) 10 months after ablation and underwent implantable cardioverter-defibrillator implantation. During an average follow-up of 30.4±29.3 months (range, 4 to 103), no patient had recurrent arrhythmia detected (including patient 7).

Discussion

We found that reentry circuit isthmuses in VT after repair of CHD are located within distinct anatomic isthmuses bordered by unexcitable tissue. The boundaries can be identified with 3D substrate mapping. Transecting anatomic isthmuses by linear RF lesions during SR abolished all inducible VTs, including poorly tolerated VTs not approachable by conventional activation mapping. Although 4 isthmuses could be identified, isthmus 1, between an area of anterior wall RVOT scar/patch and the TA, was involved in 73% of VTs in this series. The described substrate-based approach achieved long-term success for 91% of the patients.

Previous Studies

Limited information is available on mapping and ablation of VTs in patients after repair of CHD (Table 3).^{4-10,15-24} Small series reported success rates between 50% and 81% for targeting hemodynamically stable VT. More recently, an intention-to-treat analysis revealed procedural success of 50% with a 40% recurrence rate.¹⁰

Table 3. Summary of Published Mapping and Ablation Data of Patients With VT After Repair of CHD

Type of Procedure and Author, Year	CHD (n)	Method of Mapping and Ablation	Definition of Site of Origin	Patients, n	Sustained VT, n	Mean VTCL, ms
EPS						
Kugler et al, ²² 1983	TOF	3 Catheters His, RVOT, RVa, LAT	EA	3	3	216
Horowitz et al, ²⁰ 1980	TOF	AM, R intraoperative mapping (2)	EA	4	5	278
Catheter ablation†						
Burton et al, ¹⁶ 1993	TOF	PM, RFR	Exit site short S-QRS	2	2	270
Biblo et al, ¹⁵ 1994	TOF	AM, RFR	MDA	1	2	430
Goldner et al, ¹⁸ 1994	TOF	PM, RFR	Exit site short S-QRS	1	1	240
Cinushi et al, ⁴ 1995	TOF	AM, RFR linear lesion	MDA	1	2	420
Gonska et al, ⁹ 1996‡	TOF (7), VSD (1), T/VSD (1), PS (2)	AM/EM, RFR	MDA	11	11	377
Horton et al, ⁵ 1997	TOF	AM/EM, RFR linear lesion	MDA	2	2	430
Rostock et al, ²³ 2004	TOF	AM/EM, RFR C, Linear lesion	Exit site short S-QRS	1	1	340
Morwood et al, ¹⁰ 2004	TOF (8), VSD (3), Other (3)	RFR/RFR C	...	14 (20 procedures)
Furushima et al, ⁹ 2005	TOF/DORV	AM/EM, RFR linear lesion	MDA	7	14 (targeted, 8)	346
Surgical therapy ablation§						
Downar et al, ¹⁷ 1992	TOF	AM, Cryo, linear lesion	EA (exit)	4	5	240
Misaki et al, ⁶ 1994	TOF	AM, Cryo+ excision of VT origin	MDA	3	4	295
Harrison et al, ¹⁹ 1997	TOF	AM, Cryo+PVR (11)+ aneurysm-ectomy (9) linear lesions	...	14	...	261
Therrien et al, ²⁴ 2001	TOF	AM, Cryo+PVR linear lesion	Areas of slow conduction	9
Karamlou et al, ²¹ 2006	TOF	AM, Cryo+PVR linear lesion	Macroreentry site	44 (31 ablation)

(Continued)

EPS indicates electrophysiological study; VSD, ventricular septal defect; T, transposition; PS, pulmonary valve stenosis; DORV, double-outlet RV; RVa, RV apex; RV, RV inflow; LAT, local activation time; EA, earliest activation; MDA, middiastolic activation; PV, pulmonary valve; PM, pace mapping; EM, entrainment mapping; AM, activation mapping; R, roving catheter; C, CARTO; Cryo, cryoablation; PVR, pulmonary valve replacement; and NI, not inducible.

*Origin of VT mapped to an isthmus as outlined in Figure 4.

†Total short-term success for catheter ablation was 32/47, or 68%. Total recurrence was 12/36, or 33%.

‡Patients with spontaneous or induced sustained VT.

§Total recurrence for surgical therapy ablation was 7/57, or 12.3%.

In agreement with our findings, previous reports also have found VT to be due to macroreentry.^{4,5,7} Misaki et al⁶ described activation revolving around a myotomy scar with diastolic activity within the lateral RVOT wall consistent with the most common location of reentry circuit isthmuses in the present study.

Although macroreentrant may occur around obstacles in the absence of conduction delay, most studies suggest a slow-conduction area participating in the circuit. Slow conduction within an anatomic isthmus was suggested in 10 of our 11 patients by a prolonged S-QRS during pace mapping or entrainment.¹⁴ RV remodeling induced by pressure or volume load might promote hypertrophy and fibrosis with

slow conduction, providing the link between impaired hemodynamics and VT.^{25,26} However, in our series, only 2 patients had undergone a second operation for pulmonary regurgitation and 2 had moderate regurgitation. RV incision and myectomy produce RVOT aneurysmal or akinetic regions in >50% of the patients.²⁷ Misaki et al⁶ found surviving myocytes embedded in fibrous tissue in resected tissue from an RVOT region with delayed conduction, resembling the histological findings in the border zone of infarcted myocardium.⁶ Of interest, the postmortem specimen of the patient who survived 5 years after repair showed extreme thinning only of the anterolateral RVOT, consistent with isthmus 1 (Figure 4e).

Table 3. Continued

Location of Origin	Isthmus*	Short-Term Success	Reason for Failure	Follow-Up, mo	Recurrence in Ablated Patients, n (%)
RVI
RVOT
RVOT anterior, posterior	...	2/2	...	4	0/2
RVOT anterior	1	1/1	...	28	0/1
RVOT anterior	1	1/1	...	7	0/1
RV/PV	2	2/2	0/1
Scar infundibulectomy	...	9/11	EM failure	16±9	2/11
RVOT patch/TA	1	2/2	...	11	0/2
RVOT inferior PV	...	1/1	...	15	0/1
...	...	10/20	NI unstable, high-risk location	45.6±24	4/10
RVOT (3), RV septal (4)	1-2-3	4/7	Large areas of slow conduction	0.5	6/7
RVOT septal (3), RV free wall (1)	31	2/4	Cryoablation in beating heart	...	1/4
RVOT free wall/TA	1	...	NI	40	1/3
RVOT septal, RV free wall	...	10/14	NI (3), no data (1)	48±42	2/10
...	56.4	0/9
...	Multifocal (3), NI (5), no data (5)	120	3/31

Substrate Mapping

Identification of scar from voltage mapping and pace mapping is used in unmappable VTs resulting from myocardial infarction and cardiomyopathy.^{11,12,28} Voltage maps in our patients showed widely distributed low-amplitude electrograms within the RVOT. Sites identified as EUS are likely due to dense fibrosis.¹² The size of fibrotic regions identified by this method is not clear, and it may not identify narrow bands of fibrosis that also can serve as conduction block. Despite this limitation, all reentry circuit isthmuses could be assigned to an anatomic isthmus that could be transected during SR. Although we did not routinely test for conduction block across the linear lesion, completion of lesions was confirmed by noncapture with high-output pacing along the line.

The identified anatomic isthmuses were not present in all patients, consistent with the findings in postmortem specimens. Isthmus 2 was not found in the specimens, likely because of the frequent use of transannular patches. The low incidence of isthmus 4 can be explained by predominantly

perimembranous VSDs in patients with TOF. The 11 VTs sharing the anatomic isthmus 1 showed significant variation of QRS morphology. Of interest, the 2 VTs with a transition in V₂ suggesting a high septal exit were successfully ablated by transecting isthmus 3 or 4. The 2 VTs with right bundle-branch block pattern both used isthmus 2, although 1 also used isthmus 1. Thus, in unmappable VTs with a transition in V₂, ablation might target septal isthmuses, and in VTs with a right bundle-branch block pattern, targeting isthmus 2 might be justified.

Although the outcomes for our patients were good, our study cohort is a relatively small, undoubtedly selected population. Postablation management was individualized, with some patients continuing antiarrhythmic medications and some receiving implantable cardioverter-defibrillators. Sudden death can occur in patients with TOF who do not have inducible VT.²⁹ Implantation of a cardioverter-defibrillator is a reasonable consideration for many of the patients that warrants further investigation.

Study Limitations

We did not completely define reentry circuits, and >1 anatomic isthmus might be involved in a single tachycardia as demonstrated. Despite this limitation, our results provide an anatomic construct for approaching ablation. It is probable that details of the surgery importantly determine the location of reentry circuit isthmuses and may change in the future. Electrogram characteristics are likely influenced by electrode size, which varied with the mapping catheters used, but our findings of low-amplitude regions were consistent.

Conclusions

Reentry circuit isthmuses in VT after repair of CHD are located within anatomically defined isthmuses bordered by unexcitable tissue. These boundaries can be identified by 3D mapping during SR. RF ablation of the anatomic isthmus during SR is feasible and resulted in noninducibility of all VTs in our population, including those that did not allow mapping during VT. An isthmus between the TA and unexcitable tissue in the RVOT free wall was the most common cause of VT. This finding has potential implications for patients with unstable VTs and those who require repeated surgery for hemodynamic reasons, suggesting that anatomically guided ablation lesions through this isthmus are likely to interrupt VT circuits in a significant number of patients. The results should facilitate catheter and surgical ablation of VT after repair of CHD.

Disclosures

Dr Stevenson has received honoraria from Biosense Webster, Boston Scientific, Medtronic, and St Jude and has served as a consultant for Biosense Webster. The other authors report no conflicts.

References

- Murphy JG, Gersh BJ, Mair DD, Fuster V, McGoon MD, Ilstrup DM, McGoon DC, Kirklin JW, Danielson GK. Long-term outcome in patients undergoing surgical repair of tetralogy of Fallot. *N Engl J Med*. 1993; 329:593–599.
- Norgaard MA, Lauridsen P, Helvind M, Petterson G. Twenty-to-thirty-seven-year follow-up after repair for tetralogy of Fallot. *Eur J Cardiothorac Surg*. 1999;16:125–130.
- Gatzoulis MA, Balaji S, Webber SA, Siu SC, Hokanson JS, Poile C, Rosenthal M, Nakazawa M, Moller JH, Gillette PC, Webb GD, Redington AN. Risk factors for arrhythmia and sudden cardiac death late after repair of tetralogy of Fallot: a multicentre study. *Lancet*. 2000;356:975–981.
- Chinushi M, Aizawa Y, Kitazawa H, Kusano Y, Washizuka T, Shibata A. Successful radiofrequency catheter ablation for macroreentrant ventricular tachycardias in a patient with tetralogy of Fallot after corrective surgery. *Pacing Clin Electrophysiol*. 1995;18:1713–1716.
- Horton RP, Canby RC, Kessler DJ, Joglar JA, Hume A, Jessen ME, Scott WP, Page RL. Ablation of ventricular tachycardia associated with tetralogy of Fallot: demonstration of bidirectional block. *J Cardiovasc Electrophysiol*. 1997;8:432–435.
- Misaki T, Tsubota M, Watanabe G, Watanabe Y, Matumoto Y, Ishida K, Iwa T, Okada R. Surgical treatment of ventricular tachycardia after surgical repair of tetralogy of Fallot: relation between intraoperative mapping and histological findings. *Circulation*. 1994;90:264–271.
- Stevenson WG, Delacretaz E, Friedman PL, Ellison KE. Identification and ablation of macroreentrant ventricular tachycardia with the CARTO electroanatomical mapping system. *Pacing Clin Electrophysiol*. 1998;21: 1448–1456.
- Gonska BD, Cao K, Raab J, Eigster G, Kreuzer H. Radiofrequency catheter ablation of right ventricular tachycardia late after repair of congenital heart defects. *Circulation*. 1996;94:1902–1908.
- Furushima H, Chinushi M, Sugiura H, Komura S, Tanabe Y, Watanabe H, Washizuka T, Aizawa Y. Ventricular tachycardia late after repair of congenital heart disease: efficacy of combination therapy with radiofrequency catheter ablation and class III antiarrhythmic agents and long-term outcome. *J Electrocardiol*. 2006;39: 219–224.
- Morwood JG, Friedman JK, Berul CI, Khairy P, Alexander ME, Cecchin F, Walsh EP. Radiofrequency catheter ablation of ventricular tachycardia in children and young adults with congenital heart disease. *Heart Rhythm*. 2004;1:301–308.
- Marchlinski FE, Callans DJ, Gottlieb CD, Zado E. Linear ablation lesions for control of unmappable ventricular tachycardia in patients with ischemic and nonischemic cardiomyopathy. *Circulation*. 2000;101:1288–1296.
- Soejima K, Stevenson WG, Maisel WH, Sapp JL, Epstein LM. Electrically unexcitable scar mapping based on pacing threshold for identification of the reentry circuit isthmus: feasibility for guiding ventricular tachycardia ablation. *Circulation*. 2002;106:1678–1683.
- Vliegen HW, vanStraten A, deRoos A, Roest AA, Schoof PH, Zwinderman AH, Ottenkamp J, VanderWall EE, Hazekamp MG. Magnetic resonance imaging to assess the hemodynamic effects of pulmonary valve replacement in adults late after repair of tetralogy of Fallot. *Circulation*. 2002;106:1703–1707.
- Stevenson WG, Sager PT, Natterson PD, Saxon LA, Middlekauff HR, Wiener I. Relation of pace mapping QRS configuration and conduction delay to ventricular tachycardia reentry circuits in human infarct scars. *J Am Coll Cardiol*. 1995;26:481–488.
- Biblo LA, Carlson MD. Transcatheter radiofrequency ablation of ventricular tachycardia following surgical correction of tetralogy of Fallot. *Pacing Clin Electrophysiol*. 1994;17:1556–1560.
- Burton ME, Leon AR. Radiofrequency catheter ablation of right ventricular outflow tract tachycardia late after complete repair of tetralogy of Fallot using the pace mapping technique. *Pacing Clin Electrophysiol*. 1993;16:2319–2325.
- Downar E, Harris L, Kimber S, Mickleborough L, Williams W, Sevaptisidis E, Masse S, Chen TC, Chan A, Genga A. Ventricular tachycardia after surgical repair of tetralogy of Fallot: results of intraoperative mapping studies. *J Am Coll Cardiol*. 1992;20:648–655.
- Goldner BG, Cooper R, Blau W, Cohen TJ. Radiofrequency catheter ablation as a primary therapy for treatment of ventricular tachycardia in a patient after repair of tetralogy of Fallot. *Pacing Clin Electrophysiol*. 1994;17:1441–1446.
- Harrison DA, Harris L, Siu SC, Connelly MS, Webb GD, Downar E, McLaughlin PR, Williams WG. Sustained ventricular tachycardia in adult patients late after repair of tetralogy of Fallot. *J Am Coll Cardiol*. 1997;30:1368–1373.
- Horowitz LN, Vetter VL, Harken AH, Josephson ME. Electrophysiologic characteristics of sustained ventricular tachycardia occurring after repair of tetralogy of Fallot. *Am J Cardiol*. 1980;46:446–452.
- Karamlou T, Silber I, Lao R, McCrindle BW, Harris L, Downar E, Webb GD, Colman JM, VanArsdell GS, Williams WG. Outcomes after late reoperation in patients with repaired tetralogy of Fallot: the impact of arrhythmia and arrhythmia surgery. *Ann Thorac Surg*. 2006;81: 1786–1793.
- Kugler JD, Pinsky WW, Cheatham JP, Hofschire PJ, Mooring PK, Fleming WH. Sustained ventricular tachycardia after repair of tetralogy of Fallot: new electrophysiologic findings. *Am J Cardiol*. 1983;51: 1137–1143.
- Rostock T, Willems S, Ventura R, Weiss C, Risius T, Meinertz T. Radiofrequency catheter ablation of a macroreentrant ventricular tachycardia late after surgical repair of tetralogy of Fallot using the electroanatomical mapping (CARTO). *Pacing Clin Electrophysiol*. 2004; 27:801–804.
- Therrien J, Siu SC, Harris L, Dore A, Niwa K, Janousek J, Williams WG, Webb G, Gatzoulis MA. Impact of pulmonary valve replacement on arrhythmia propensity late after repair of tetralogy of Fallot. *Circulation*. 2001;103:2489–2494.
- Deanfield J, McKenna W, Rowland E. Local abnormalities of right ventricular depolarization after repair of tetralogy of Fallot: a basis for ventricular arrhythmia. *Am J Cardiol*. 1985;55:522–525.
- Marie PY, Marcon F, Brunotte F, Briancon S, Danchin N, Worms AM, Robert J, Pernot C. Right ventricular overload and induced sustained ventricular tachycardia in operatively “repaired” tetralogy of Fallot. *Am J Cardiol*. 1992;69:785–789.
- Davlouros PA, Kilner PJ, Hornung TS, Li W, Francis JM, Moon JC, Smith GC, Tat T, Pennell DJ, Gatzoulis MA. Right ventricular function in adults with repaired tetralogy of Fallot assessed with cardiovascular

- magnetic resonance imaging: detrimental role of right ventricular outflow aneurysms or akinesia and adverse right-to-left ventricular interaction. *J Am Coll Cardiol*. 2002;40:2044–2052.
28. Arenal A, del Castillo S, Gonzalez-Torrecilla E, Aienza F, Ortiz M, Jimenez J, Puchol A, Garcia J, Almendral J. Tachycardia-related channel in the scar tissue in patients with sustained monomorphic ventricular tachycardias: influence of the voltage scar definition. *Circulation*. 2004;110:2568–2574.
29. Alexander ME, Walsh EP, Saul JP, Epstein MR, Triedman JK. Value of programmed ventricular stimulation in patients with congenital heart disease. *J Cardiovasc Electrophysiol*. 1999;10:1033–1044.

CLINICAL PERSPECTIVE

Ventricular scars from surgical repair of congenital heart disease are a source of ventricular tachycardia (VT) causing late morbidity and sudden death. The increasing number of patients with corrected congenital heart disease who are entering the adult population is likely to increase the number of patients who require treatment for VT. Implantable cardioverter-defibrillator therapy is effective for terminating VTs, but additional therapy to prevent episodes and to reduce implantable cardioverter-defibrillator shocks is required in some patients. Catheter ablation offers the potential for preventing VT recurrences, but relatively few data exist describing reentry circuit locations and approaches to ablation. In this study, we used 3-dimensional electroanatomic reconstructions to characterize the locations of potential critical isthmuses for reentry circuits in a series of 11 patients after repair of tetralogy of Fallot or ventricular septal defect. The mapping data also were related to morphological analyses of postmortem specimens with repaired tetralogy of Fallot. We describe 4 locations for reentry circuit isthmuses. In most patients, ≥ 1 VTs involved an anatomic isthmus between the tricuspid valve annulus and an area of scar or patch in the free wall of the right ventricle. Importantly, these isthmuses can be identified during sinus rhythm. Targeting the anatomic isthmuses during sinus rhythm, radiofrequency ablation abolished all inducible VTs and led to long-term success for 91% of our patients. These findings should facilitate catheter and surgical ablation as additional antiarrhythmic therapy in selected patients with recurrent VT late after repair of congenital heart disease.